IMPLEMENTATION OF ACCURATE LUMPED PARAMETER SUBMODELS IN THE TRANSIENT THERMAL ANALYSIS OF THE ARES I UPPER STAGE THRUST VECTOR CONTROL HYDRAULIC SYSTEM

Robert J. Christie, Caleb D. Fisher
NASA Glenn Research Center

ABSTRACT

Ares I is the crew launch vehicle being developed by NASA and is specifically designed to launch the Orion crew vehicle. The Upper Stage of Ares I is propelled by the Pratt & Whitney Rocketdyne J-2X engine, and NASA Glenn Research Center is developing the Thrust Vector Control (TVC) system that will steer the vehicle during powered flight. A thermal analysis of the TVC hydraulic system was needed to ensure that proper thermal conditioning occurs prior to launch and that overheating does not occur during flight. The model of the TVC hydraulic system was created with SINAPS® which is a graphical user interface for SINDA/FLUINT; and the thermal boundary conditions were generated by a thermal model of the Ares I Upper Stage Aft Compartment, which was developed at Marshall Space Flight Center using Thermal Desktop®. Several finite element method and computational fluid dynamic models were created using ANSYS Workbench® and CFdesign®, for the purpose of conducting detailed analyses at the component level. Results from these models were used to adjust the simplified lumps of the SINAPS system-level model until it behaved similarly to the component-level models. SINAPS component characterization was also correlated to breadboard test data. This analysis demonstrated how finite element methods, computational fluid dynamics, and reduction of test data can all be utilized to develop simple lumped-parameter models that mimic the output of more complex analysis models; and these simplified representations can then be integrated into a system-level model without any computational performance penalty.

INTRODUCTION

Ares I, shown in Figure 1, is a two-stage rocket topped by the Orion crew exploration vehicle. The first stage is a single, five-segment, solid propellant, reusable booster. The second stage is propelled by a J-2X engine fueled with liquid oxygen and liquid hydrogen and is being designed by Marshall Space Flight Center (MSFC). The thrust vector direction of the J-2X engine is controlled by the Thrust Vector Control (TVC) system being designed at Glenn Research Center (GRC).

® SINAPS is a registered trademark of Cullimore & Ring Technologies
® Thermal Desktop is a registered trademark of Cullimore & Ring Technologies
® ANSYS Workbench is a registered trademark of ANSYS, Inc.
® CFdesign is a registered trademark of Blue Ridge Numerics, Inc.

All of the components of the TVC system are mounted on the Thrust Cone of the Upper Stage. The Thrust Cone is located in the Aft Compartment and is attached to the liquid oxygen (LOX) propellant tank. The Upper Stage Aft Compartment is shown in Figure 2. Since the Thrust Cone is attached to the LOX tank, it can reach temperatures near -300^{o}F after propellant is loaded. These cold temperatures were a major concern during the design of the TVC system.

The purpose of the TVC subsystem is to gimbal the J-2X main engine during upper stage (US) ascent. Two hydraulic actuators steer the J-2X engine in response to commands from the flight computer; one actuator controls the "Rock" axis and the other controls the "Tilt" axis at a maximum rate of 5 degrees per second.

Two separate but identical hydraulic power circuits are employed. Both hydraulic power circuits incorporate a turbine pump assembly (TPA), powered by either gaseous helium or gaseous hydrogen supplied from the upper stage Main Propulsion System (MPS). The propellant is used to spin a turbine that drives a variable displacement axial piston pump through a gearbox. For ground checkouts, pad operations, and during first stage pre-separation, helium propellant will be used to drive the TPA. During J-2X operation, gaseous hydrogen drives the TPA.

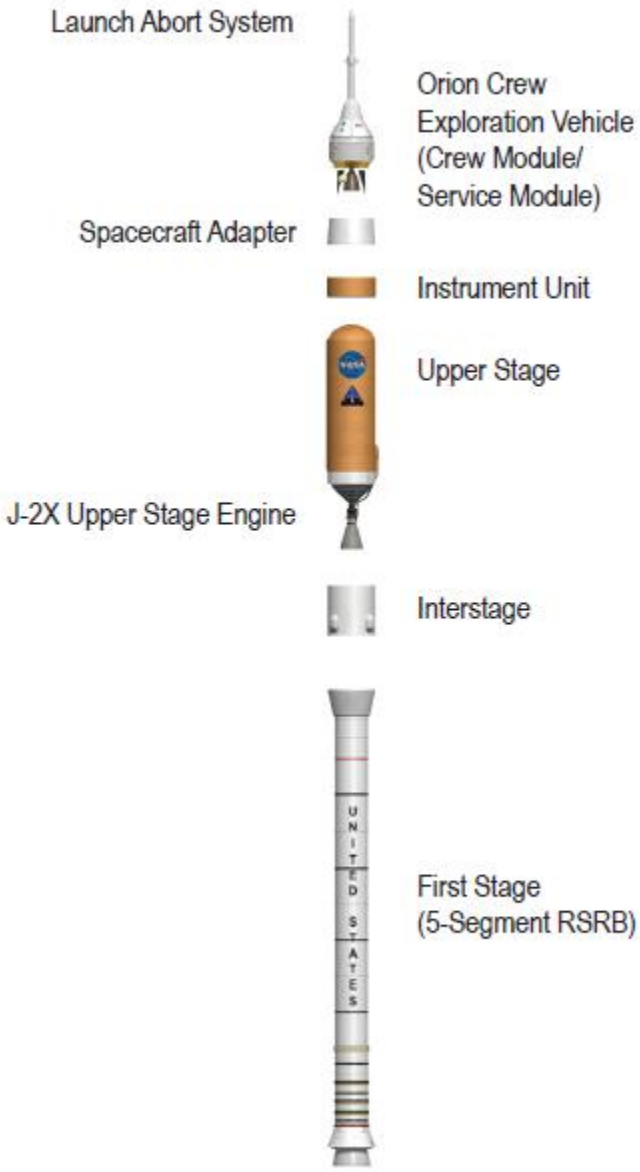

Figure 1, Ares I

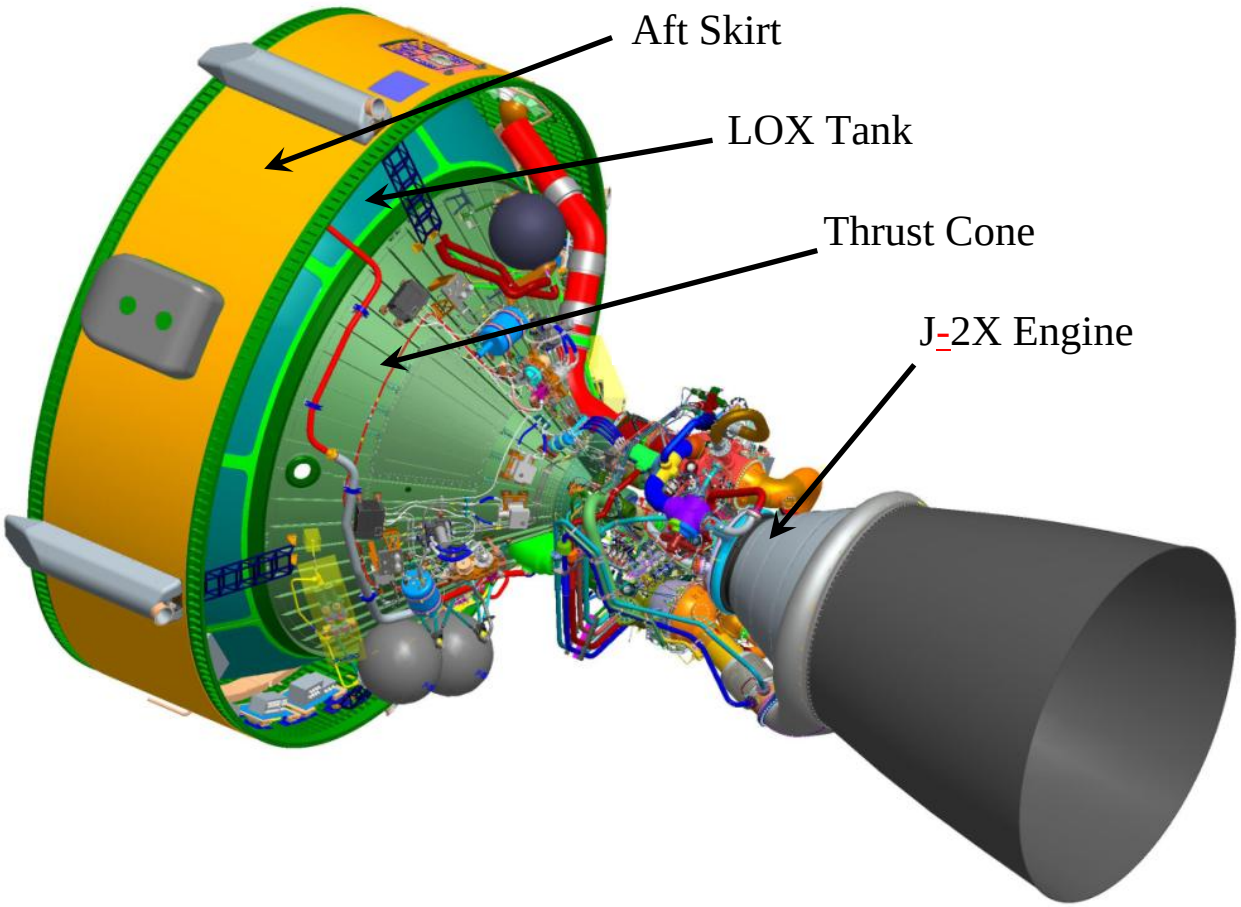

Figure 2, Ares I Upper Stage Aft Compartment

The major components of the TVC hydraulic system (shown in Figure 3) are:

- Data and Control Unit (DCU)
- Turbine Pump Assembly (TPA – consists of the Turbine, Gearbox, Pump and Mechanical Speed Control)
- Propellant Supply Valves
- Propellant Distribution Assembly
- Actuators including the following components: Flushing Valve, Selector Valve, Filters, Power Valve, Lock Valve, Torque Motors, Linear Variable Differential Transformer - LVDT actuator position indicators, Lock Valve position indicators and differential pressure sensors.
- Thermal Conditioning (includes the two Circulation Pumps and associated instrumentation)
- Hydraulic System including the Accumulator, Reservoir, Filter Manifold Assembly, Hydraulic lines, and associated instrumentation (Temperature, Pressure Sensors, Pressure Switch)

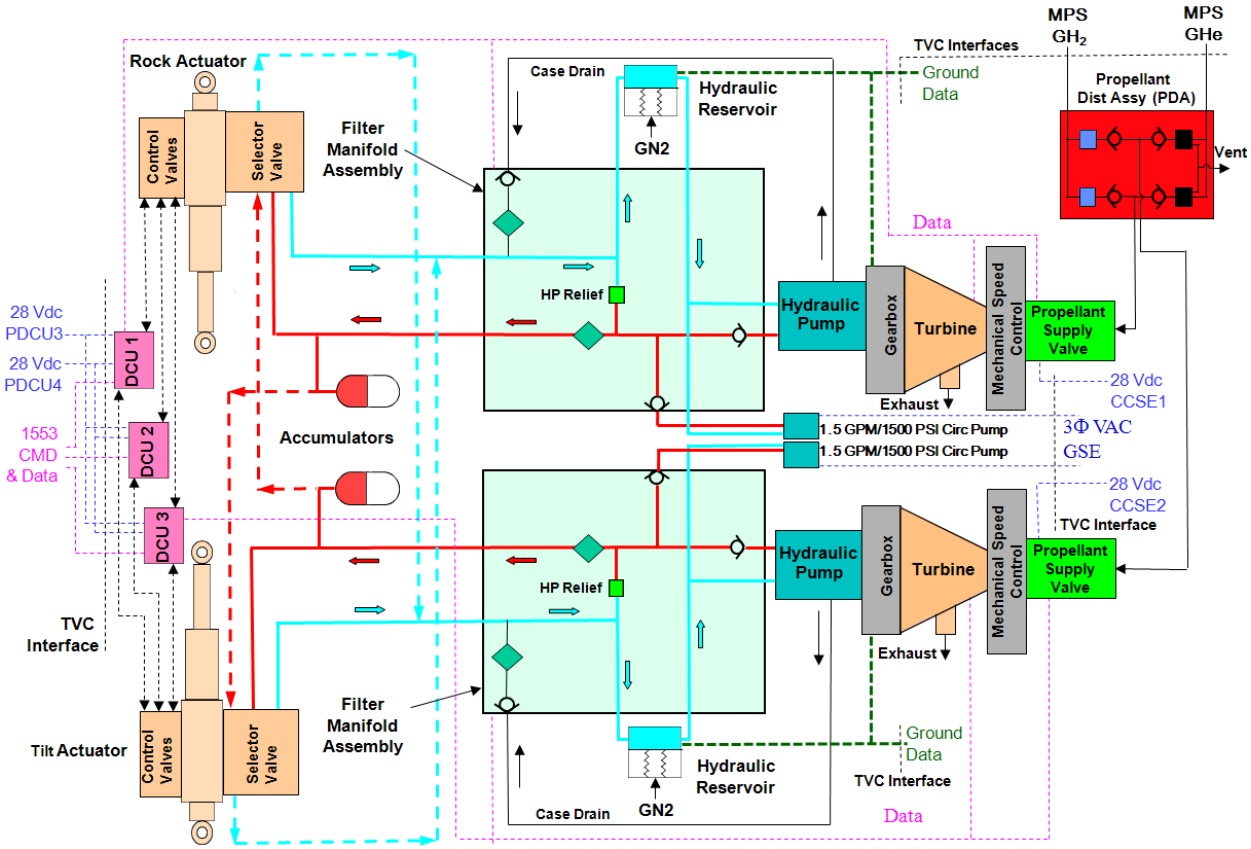

Figure 3, Thrust Vector Control Hydraulic System

The Thrust Cone is covered by a Thermal Blanket which protects its components from aerodynamic heating and plume impingement during flight. During prelaunch operations an inert purge gas is circulated between the Thrust Cone and Thermal Blanket which provides moderate heating and helps mediate the effects of the cold Thrust Cone. Additional thermal conditioning is provided to TVC hardware by intermittently running the two circulation pumps. The excess heat generated by the pumps heats the hydraulic fluid which is circulated throughout the system.

The thermal conditioning system operates the circulation pumps every 6 minutes, with the second pump lagging the first pump by 3 minutes. The timing is shown in Figure 4. Both actuators receive fluid flow when either circulation pump is operating because the actuators are "cross-strapped". The circulation pumps only operate simultaneously if their duty cycle exceeds 50%. The pumps will be started when chill-down of the LOX tanks begins and a PID controller will vary the duty cycle to achieve the desired TVC reservoir fluid temperature.

The transient thermal model of the TVC hydraulic system was modeled with SINAPS, which uses SINDA/FLUINT for its solver. The governing equations for FLUINT are provided in the Appendix. The model was used to predict the hydraulic fluid and component temperatures during all phases of system operation, with emphasis on prelaunch thermal conditioning and flight. The system-level model is shown Figure 5. Figure 6~~Figures 6~~ & 7 provide a close-up view of one of the independent circuits.

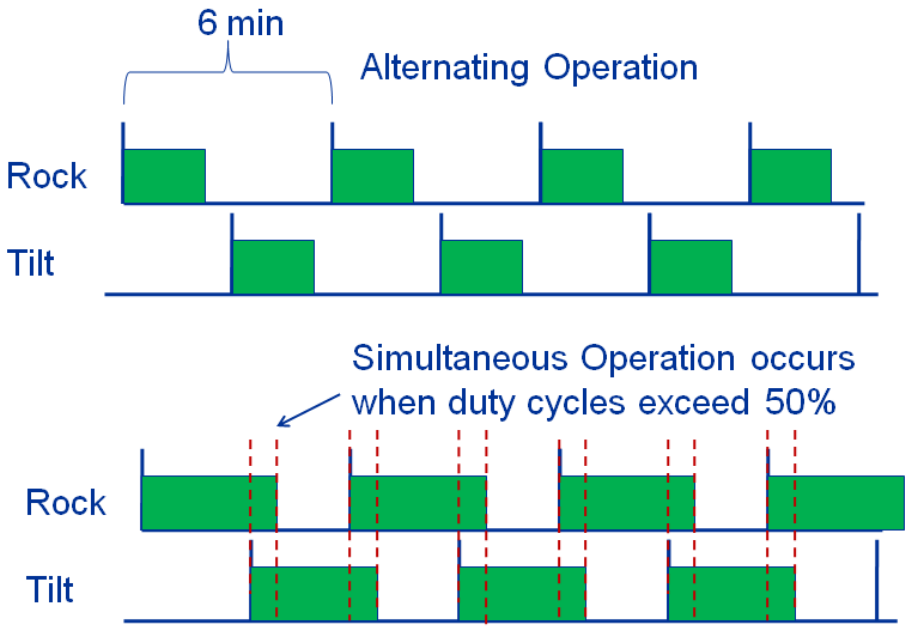

Figure 4, Circulation Pump Duty Cycles

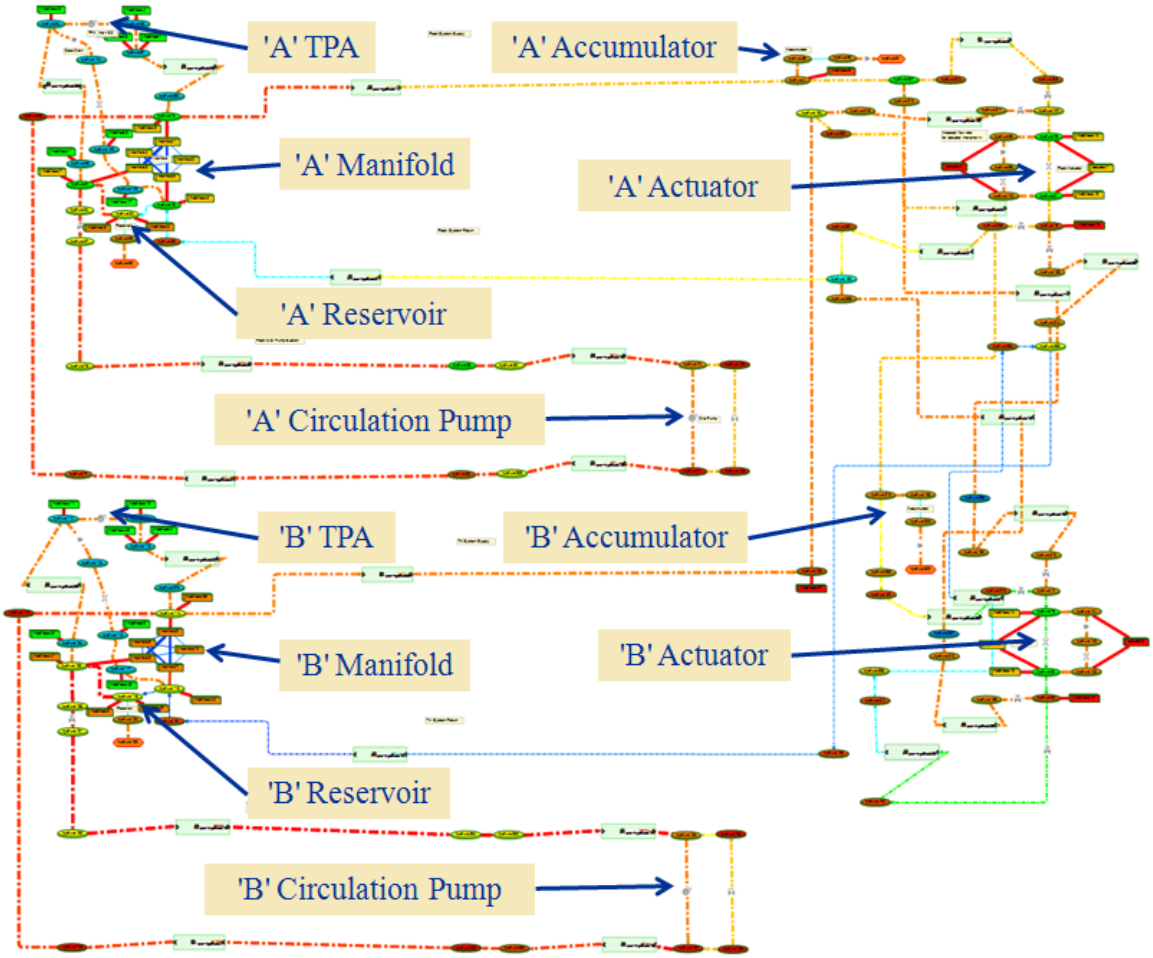

Figure 5, SINAPS Model of the TVC Hydraulic System

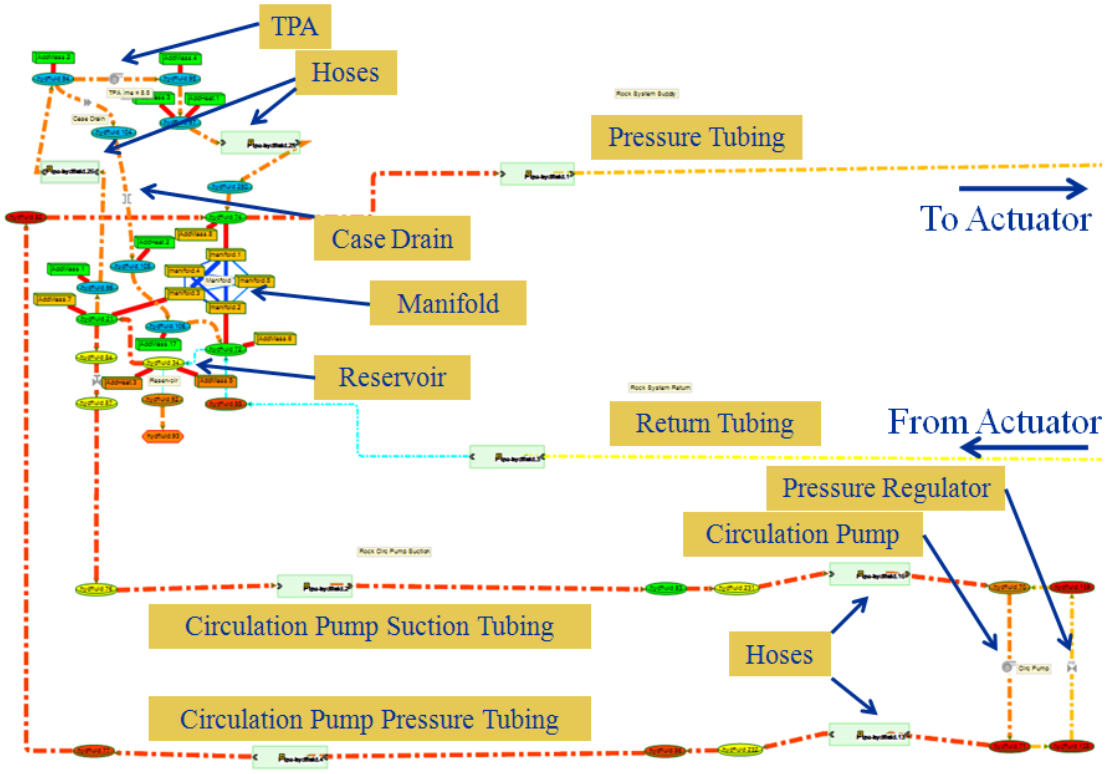

Figure 6, SINAPS Model of TVC 'A' System

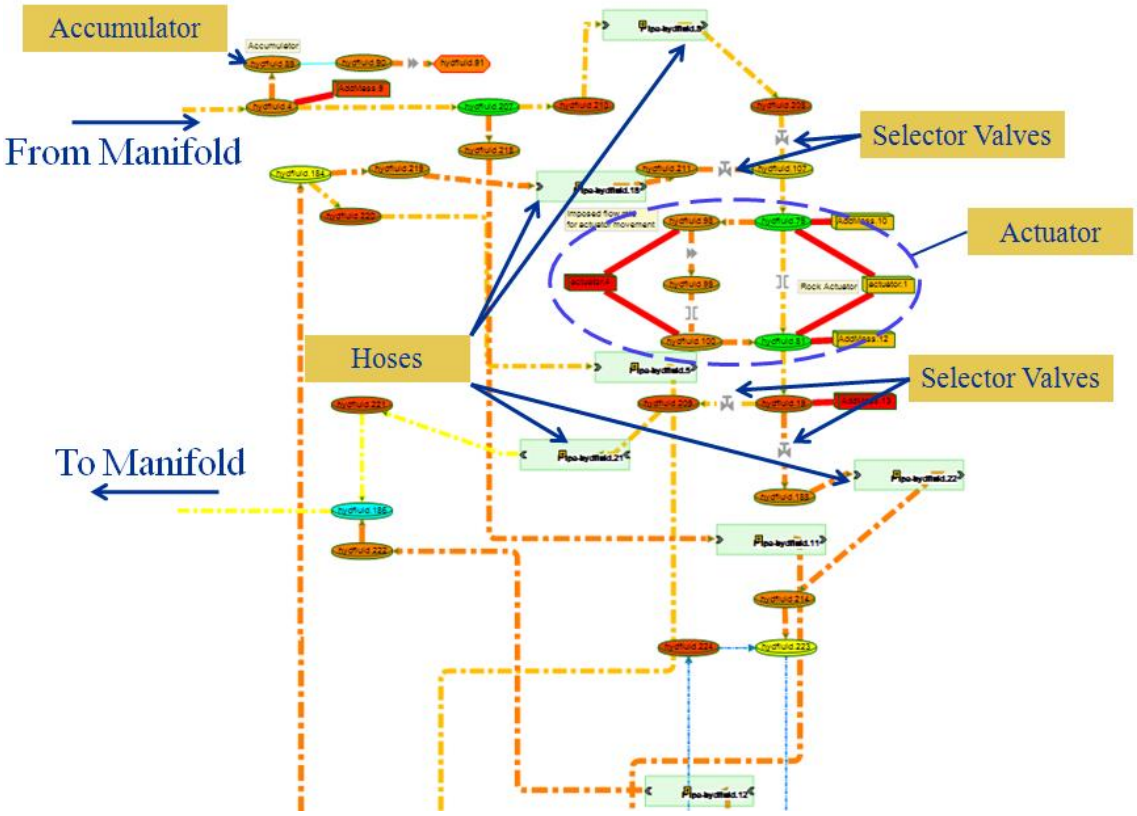

Figure 7, SINAPS Model of TVC 'A' System

These diagrams only show the fluid circuit; the model also includes convection to the purge gas, radiation to the Thrust Cone and Thermal Blanket, and conduction through the support structures. Figure 8 shows an example of the actuator inlet temperature during the final thermal conditioning cycle, during the gimbal-check 6.5 minutes prior to launch, and during the flight ascent segment, which only lasts 10 minutes.

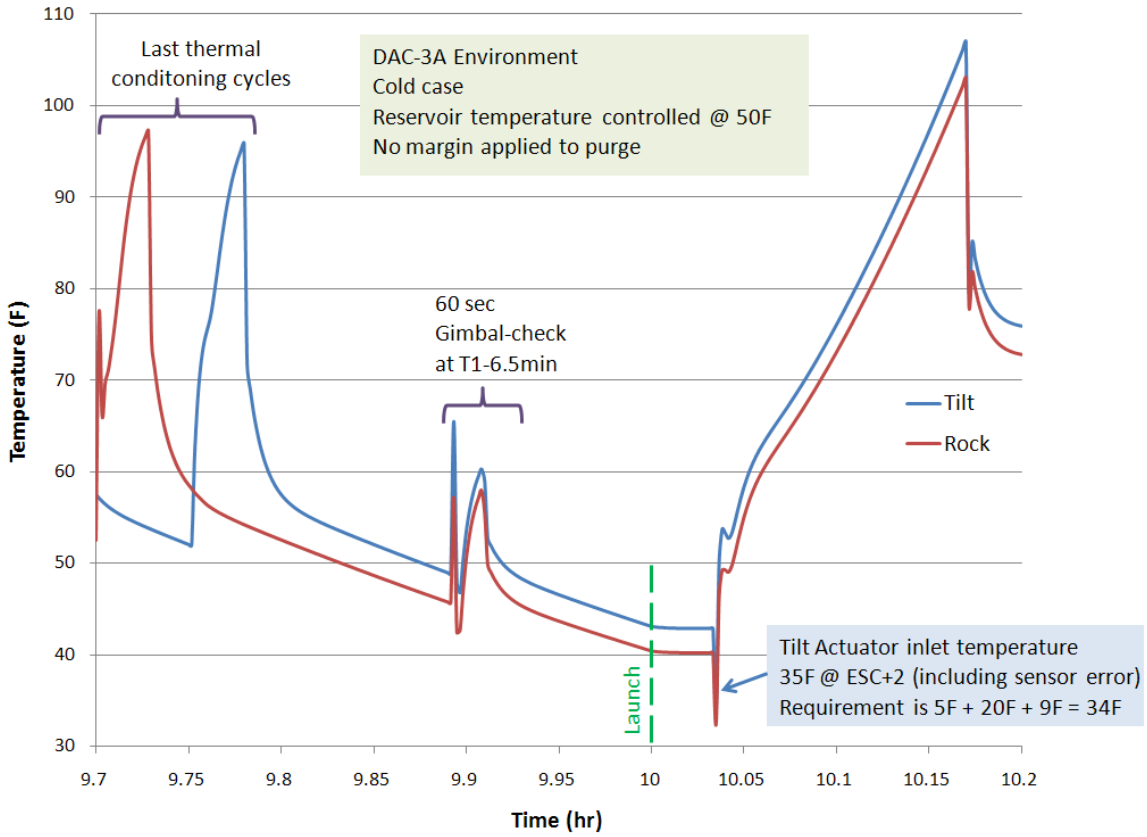

Figure 8, Example of Actuator Inlet Fluid Temperatures

COMPONENT MODELING

Several of the TVC hydraulic system components required integrated modeling methods. In several cases, the components were first analyzed with ANSYS Workbench and then were transformed into a lumped parameter of the system-level SINAPS model. The lumped parameters of the SINAPS model were adjusted until their behavior mimicked those of the FEM models. The components that this approach was applied to (in order of increasing complexity) included: Tube Supports, Actuator Hose Bracket, Filter Manifold, and Hydraulic Actuator. Additionally, the SINAPS model of the TPA Hydraulic Pump was based mainly upon test data, and the Bellows Reservoir model was based upon CFD analysis.

The simplest models to develop were those of the Tube Support, Circulation Pump Distribution Panel and the Actuator Hose Bracket with Accumulator Mount. In each case a FEM model was made using ANSYS Workbench, boundary conditions were applied and the interface reactions

were solved. A simplified lumped-parameter (LP) model was then created within SINAPS and provided the same transient response as the FEM. Figure 9 shows the FEM and the LP models of these three supports. It was found that the effective thermal mass of the all the tube mounts was less than 1% of thermal capacity of the entire hydraulic system. Similar simplifications were done for the DCU Mounts, Reservoir Supports, and numerous tube fittings. The effective thermal mass of a typical tube fitting was 30% to 33% of the mass of the fitting not including the hex nuts.

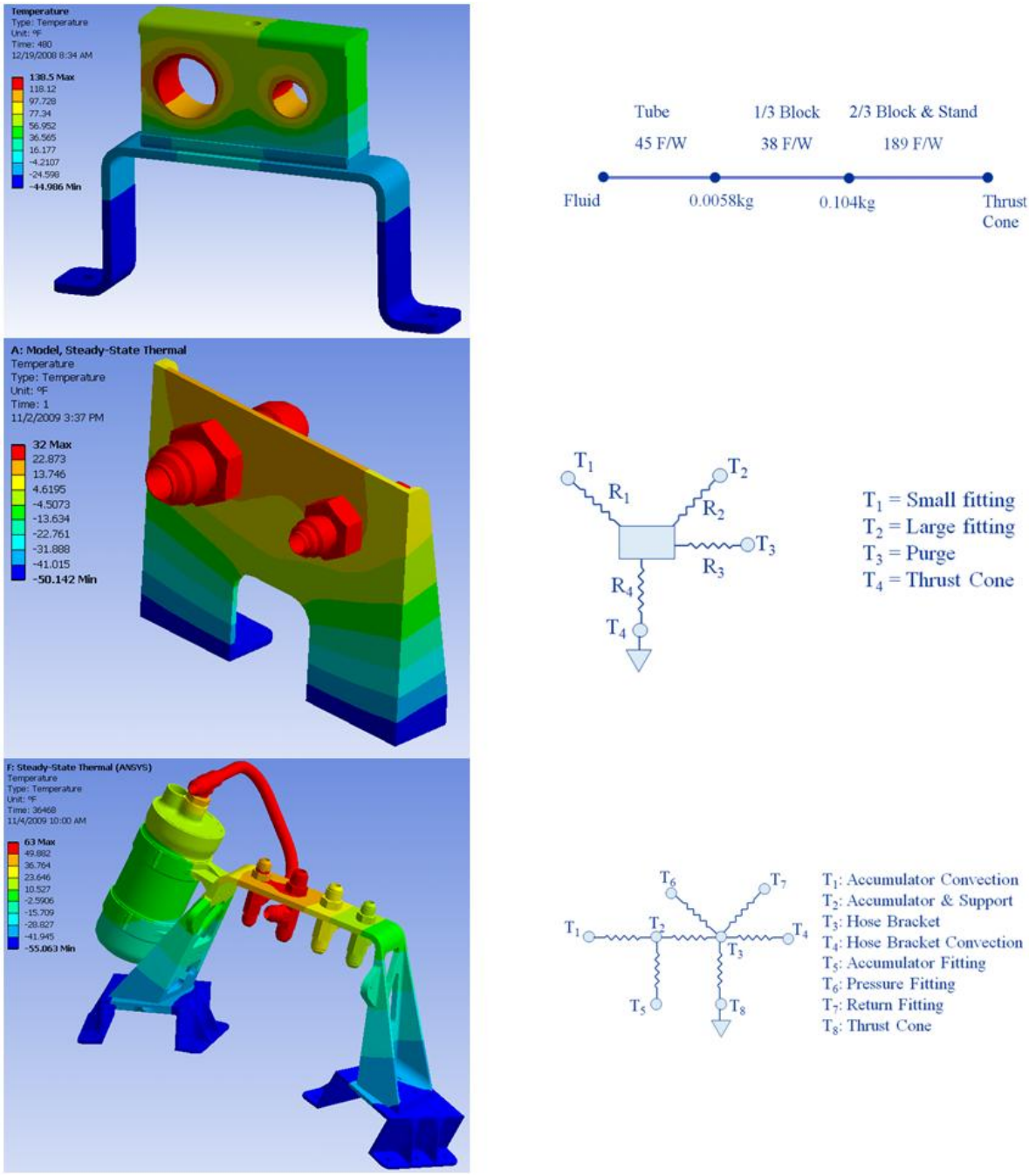

Figure 9, FEM and LP Models of Supports

FILTER MANIFOLD

The Filter Manifold is a complex body of fluid passages, and it was necessary to determine the thermal conductance of the block between the major flow passages and its transient effective thermal mass. To accomplish this, a finite element model was made (Figure 10), then a simplified network was created (Figure 11). Fixed boundary conditions were applied to the flow passages of the FEM model two at a time, and the thermal conductance of the manifold block between the pairs of passages was calculated. The internal heat transfer coefficients were calculated using equations for short duct flow. From this a SINDA model was made that had thermal conductance characteristics very similar to that of the finite element model. The resulting SINDA network is shown in Figure 12.

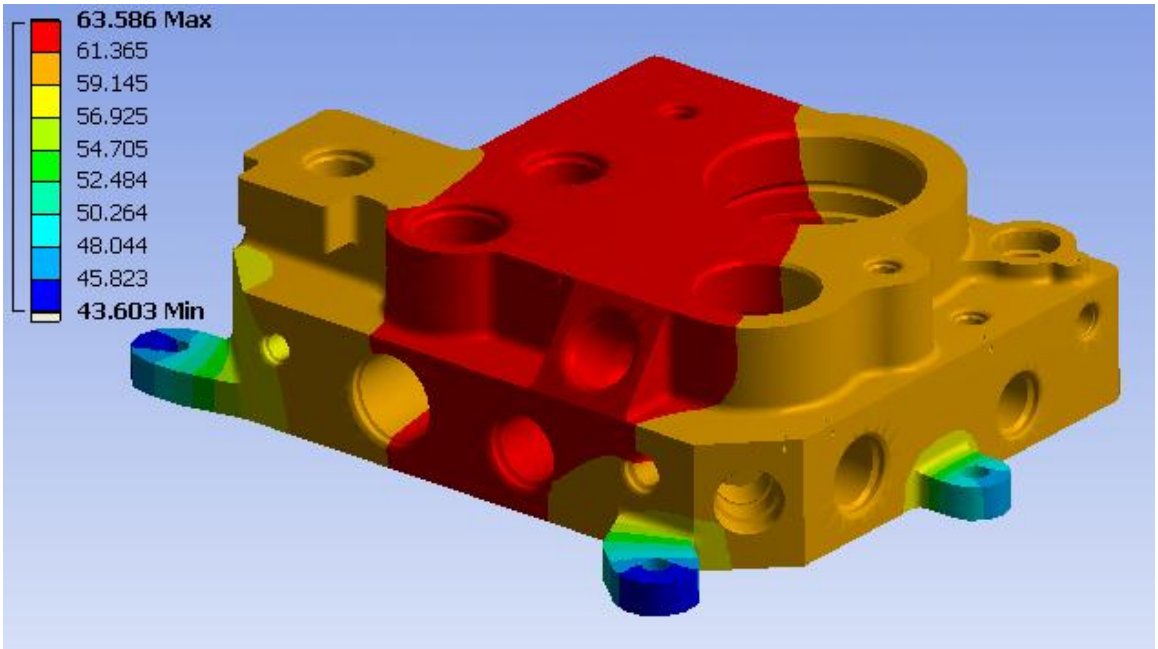

Figure 10, Finite Element Model of Filter Manifold

The next step was to assign the proper amount of thermal mass (heat capacity) to the nodes of the SINDA model. To achieve this, the flow through the passages was given a step change in temperature and the heat flow from each passage was recorded. In order to differentiate the transient portion of the heat absorbed from the linear conduction portion, the analysis was performed with the specific heat set to its proper value and then with it set to zero. Thus the first analysis provided the total heat absorbed, whereas the second analysis provided just the linear conduction. By subtracting the two, the transient portion of the heat absorbed by the thermal mass was determined.

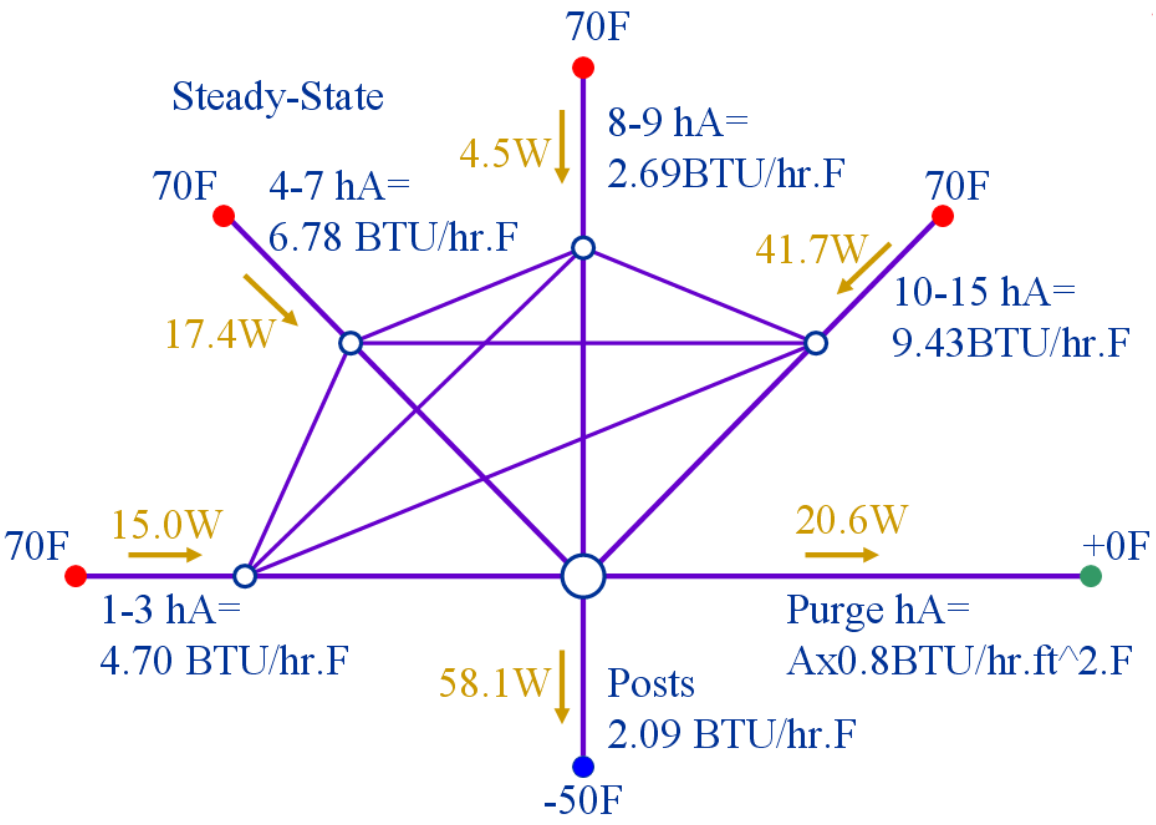

Figure 11, Lumped Parameter Model of Filter Manifold

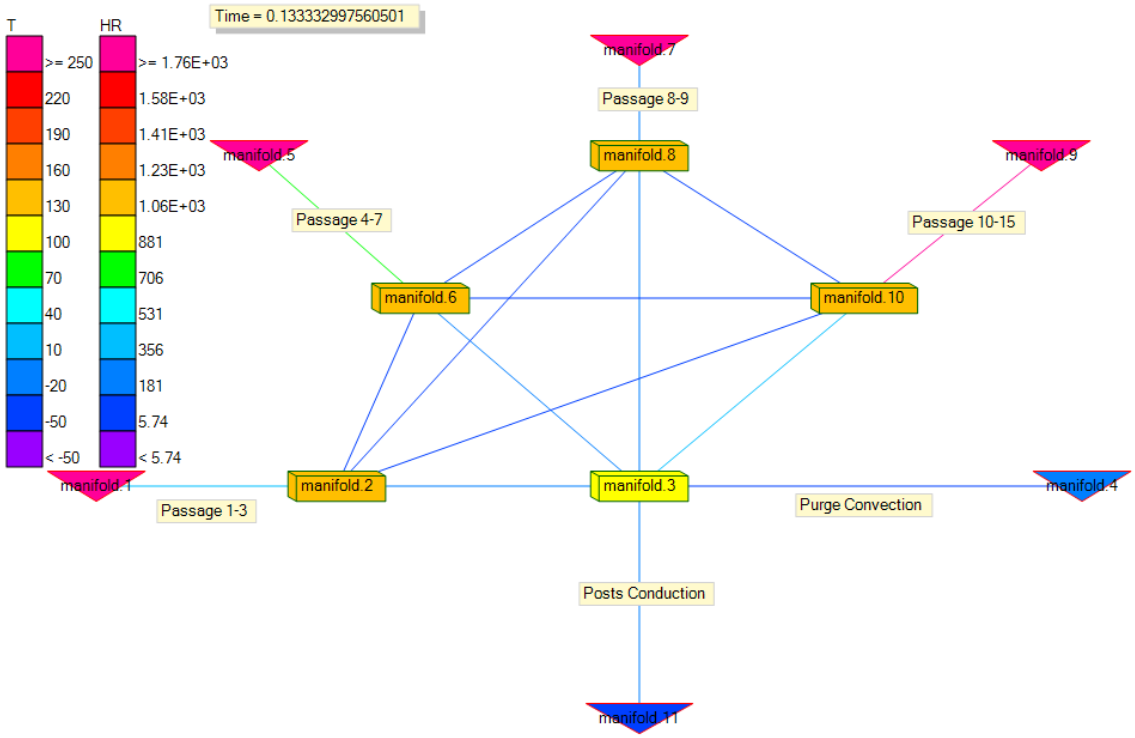

Figure 12, SINDA Network of Filter Manifold

The approach described above could not be used for the thermal mass of the node labeled as 'manifold.3' in Figure 12, because it is not in direct contact with a flow passage. So a trial and error method was used. After several iterations a good distribution of thermal mass was found. A comparison of the FEM model and the lumped-parameter model is shown in Table 1, which shows that the transient heat absorbed by the four major passages of the lumped model are within 4% of that of the FEM model.

Table 1, Comparison of Heat Absorbed

Passage	Lumped Parameter Model Absorbed Heat (kJ)	FEM Model Absorbed Heat (kJ)	Lumped Parameter Model % of total	FEM Model % of total
1-3	45	58	15	19
4-7	64	65	22	22
8-9	26	16	9	5
10-15	158	159	54	54
Subtotal	292	296	100	100
Posts	-36	-35		
Purge	-15	-15		
Total	241	246		

HYDRAULIC ACTUATOR

The hydraulic actuator also has a maze of flow passages, and the approach to simplify its lumped-parameter representation was similar to that of the filter manifold. In this case, the flow through the FEM was ramped from 60^{o}F to 250^{o}F over 8 minutes and the thermal mass of the lumped parameter model was adjusted until the thermal response matched that of the FEM model (Figure 13). The response matched when the lump's thermal mass was equivalent to 9.45 lbs. This is only 10% of the total weight of the actuator, indicating that only a small percentage of the actuator mass effectively absorbs heat from the hydraulic fluid when the actuator is not moving. When the actuator is not moving, the only flow through the actuator is the small flow required by the electro-hydraulic servo valves. That flow was simulated by the orifice in the center of Figure 14. When the actuator moves, additional flow goes through the hydraulic cylinder and the effective thermal mass increases to 25%. To accommodate this additional flow, a second orifice was added along with an additional mass which is only exposed to this additional flow. These are shown on the left side of Figure 14. Another comparison was made between the two models during a simulated 30-second gimbal check. That comparison (shown in Figure 15) shows that the transient heat absorbed by the two models is very similar.

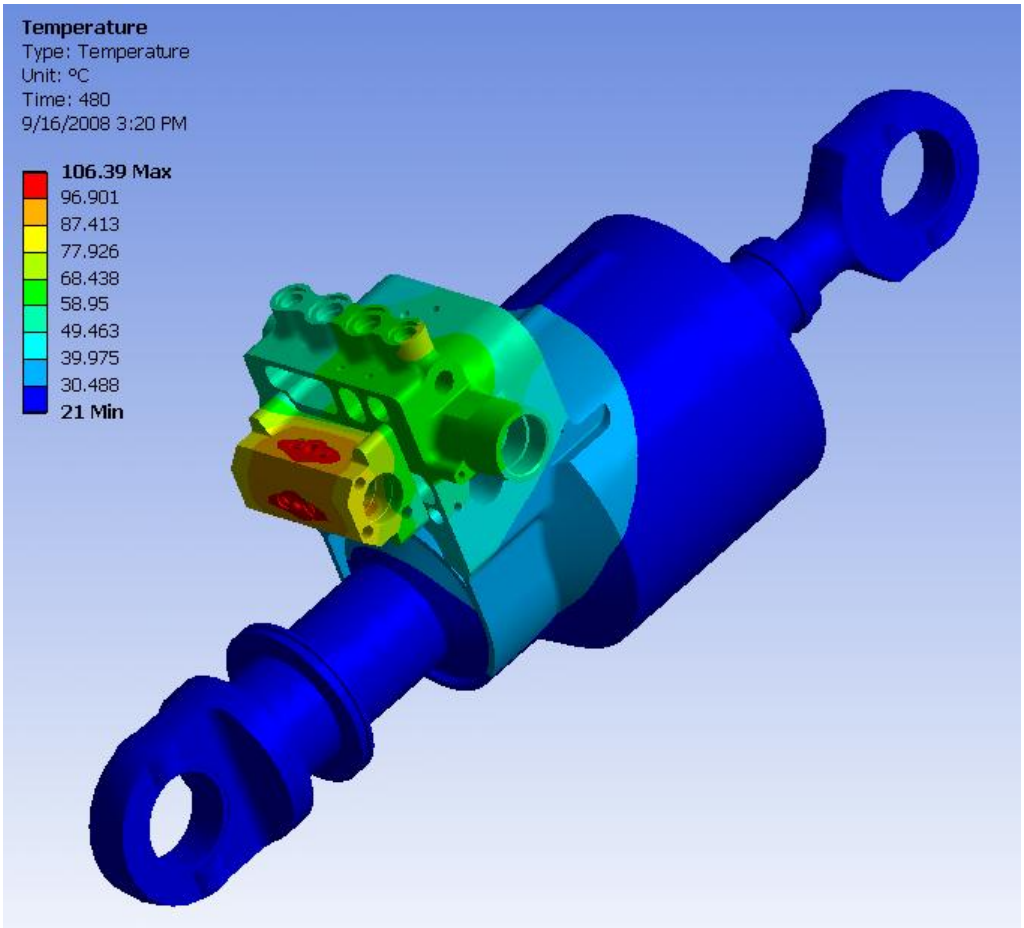

Figure 13, FEM Model of Hydraulic Actuator

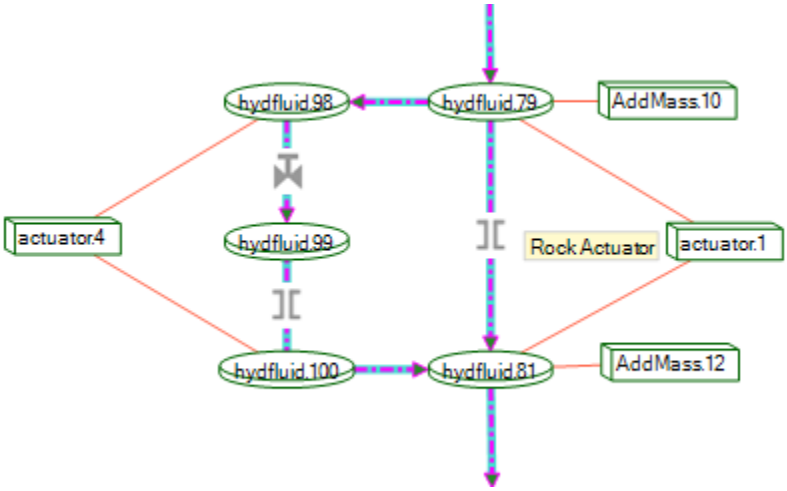

Figure 14, Lumped Parameter Model of Hydraulic Actuator

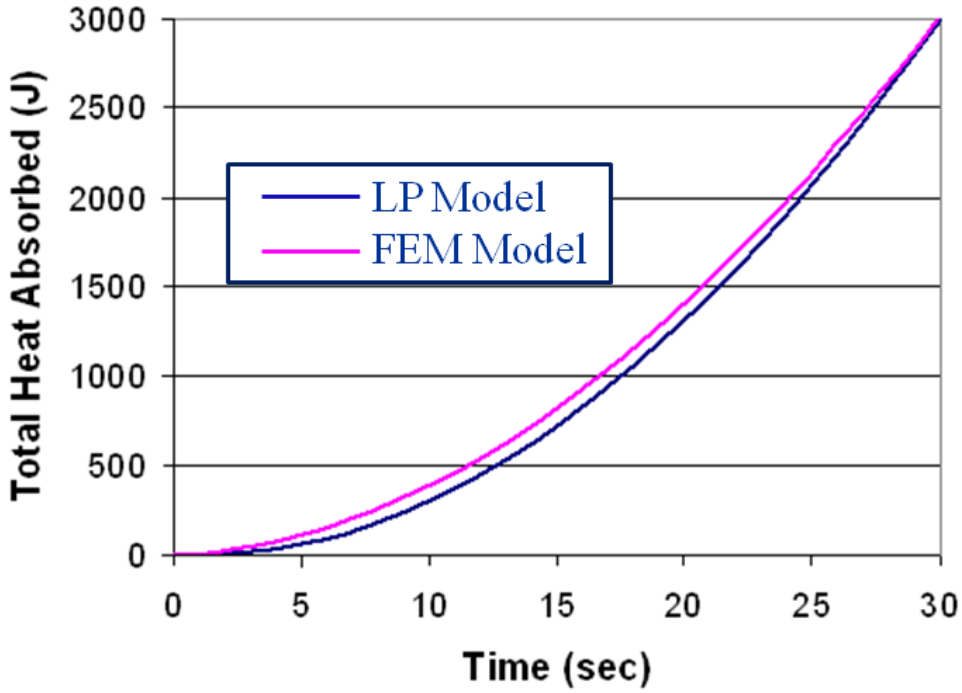

Figure 15, Heat Absorbed by Actuator During 30 second Gimbal Check

TPA PUMP

The hydraulic pump was modeled in FLUINT using the standard PUMP flow device. When using this device, the heat generated due to pump inefficiencies is dumped into the discharge flow. But in a variable displacement pump, a large portion of the heat generated by the pump leaves through the case drain flow. To account for this, the case drain flow and the associated heat loss needed to be modeled as well. The case drain flow-rate was estimated from the breadboard test data, which showed that case drain flow was increasing with time (Figure 16). This is caused by the changes in fluid viscosity and hardware clearances that both occur with changes in temperature. It was found that the case drain flow rate varied with absolute temperature and was proportional to temperature raised to the 4.4th power ($T^{4.4}$). Manufacturer's test data shows that case drain rate is also a function of main discharge flow rate. The case drain flow was included in the model by adding a "set mass flow rate" device and an orifice in parallel with the pump (Figure 17). In this configuration, the orifice counteracts the energy added by the "set mass flow rate" device.

Test data also revealed that approximately 77% of the heat generated is taken out by the case drain flow. To simulate this, the total power used by the pump was fetched from a table in FLUINT. Then using the pump efficiency curve, the heat generated was determined. 77% of that was subtracted from the discharge flow and added to the case drain flow. The effective thermal mass of the pump was also added to the case drain flow path. By trial and error it was found that 100% of the pump's thermal mass was needed. Figure 18 shows a comparison between the case drain temperature of the FLUINT model and the equation that fits the test data and shows there is a good fit for the period of interest.

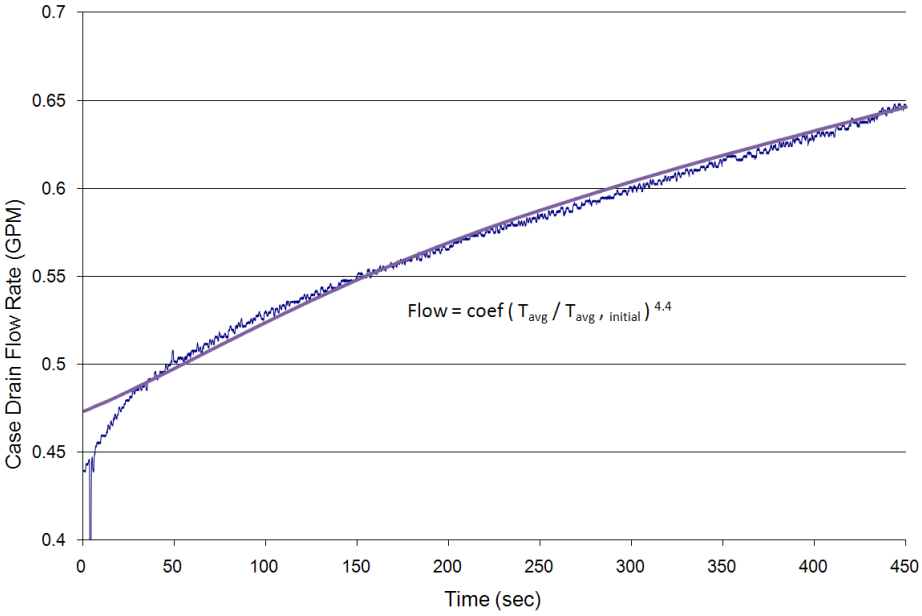

Figure 16, Case Drain Flow During TVC Breadboard Test

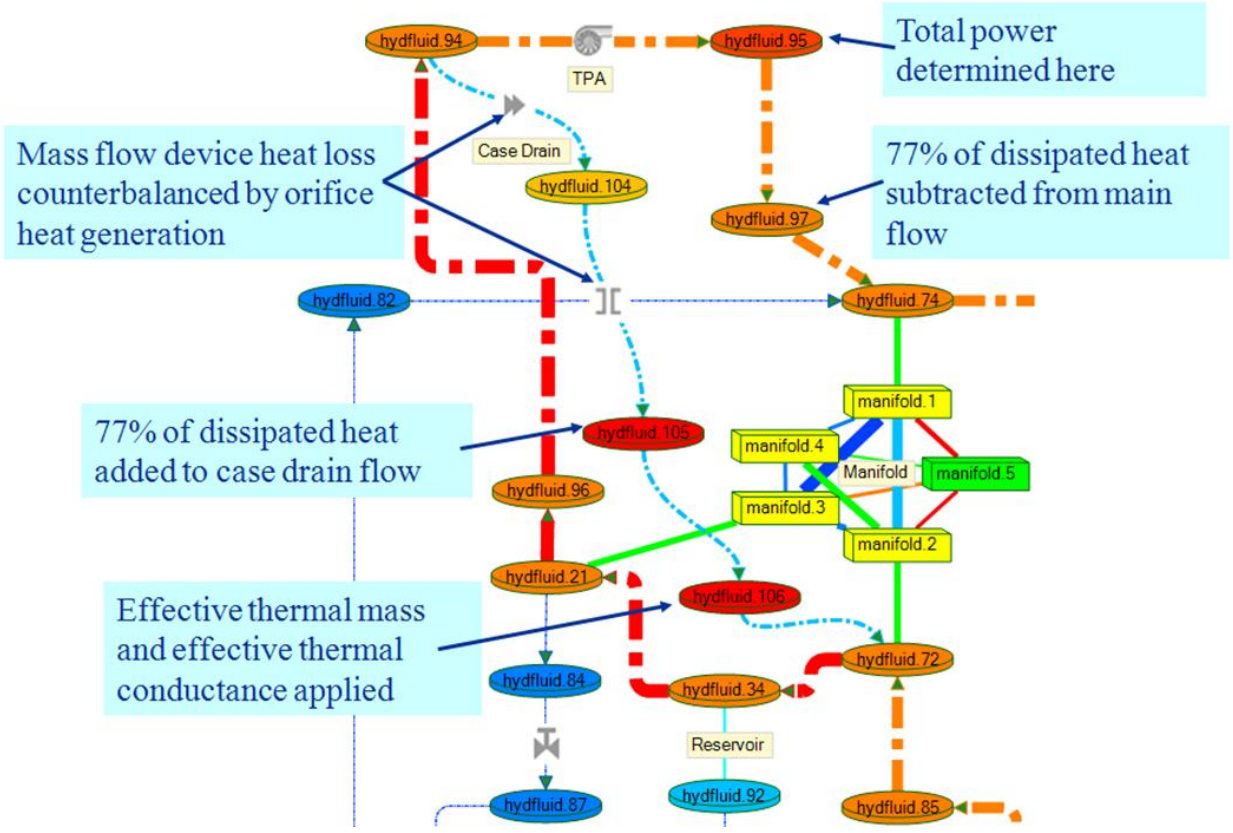

Figure 17, FLUINT Model of TPA Hydraulic Pump

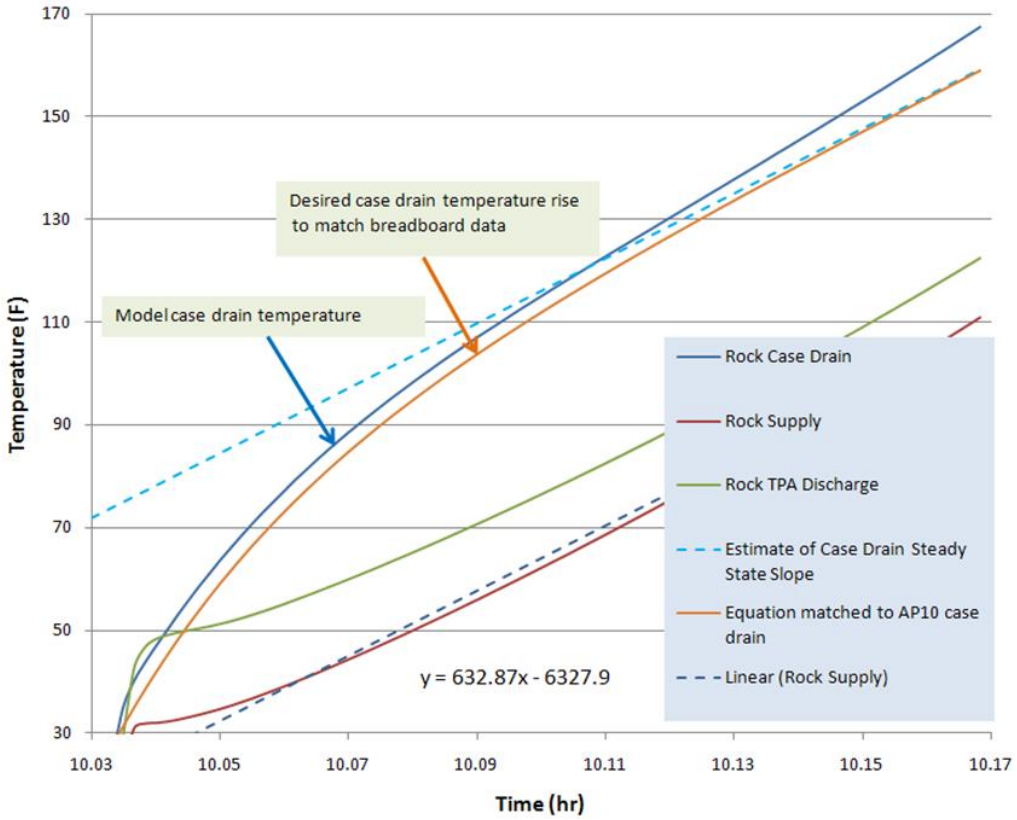

Figure 18, Comparison of Model Case Drain Temperature vs. Test Data

BELLOWS RESERVOIR

During flight the heat generated by the TVC hydraulic system is mainly absorbed by the hydraulic fluid, most of which resides in the Reservoir. Therefore, it was necessary to have an accurate value for the effective thermal mass of the Reservoir. During pump operation, the temperatures in the Reservoir are not homogenous and some warm fluid exits the Reservoir before complete mixing occurs. To account for this thermal behavior, a CFD model was made of the Reservoir using CFdesign (Figure 19). A typical flight mission was simulated and the total heat absorbed by the Reservoir was calculated. The CFD analysis determined that the Reservoir's effective thermal mass was 83% of its actual total thermal mass. This effective thermal mass was then used in the Transient Thermal Model of the TVC Hydraulic System (shown earlier in Figure 5) and its response was compared to that of the CFD model. The comparison is shown in Figure 20, which shows good correlation between the complex CFD model and the single node SINDA/FLUINT model.

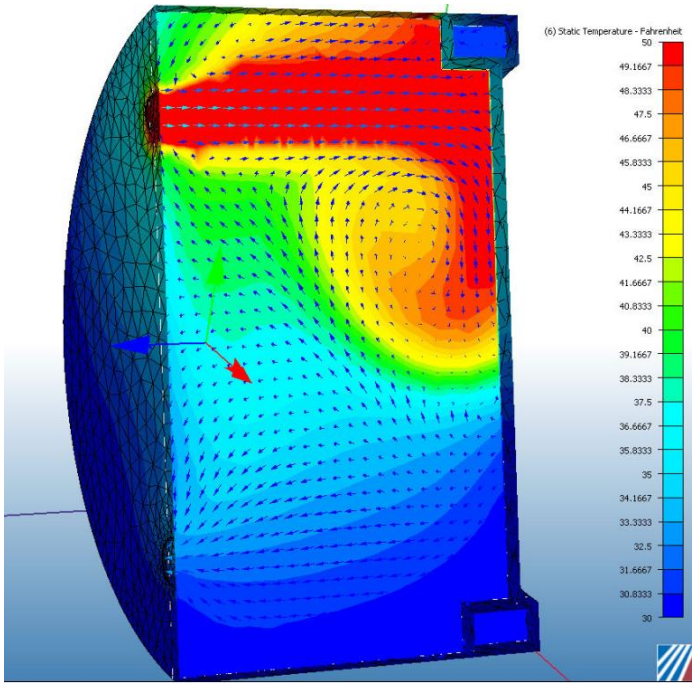

Figure 19, CFD Model of Reservoir Fluid

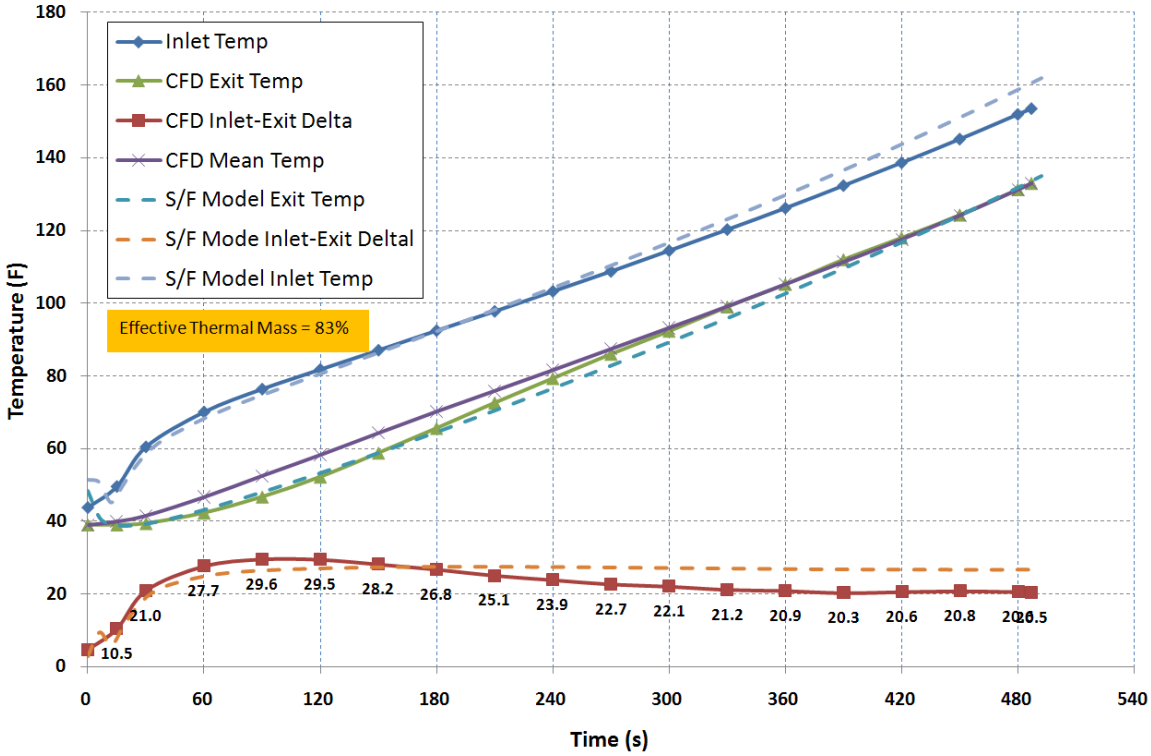

Figure 20, Comparison of CFD Model and LP Model of Bellows Reservoir

CONCLUSIONS

This project has demonstrated how finite element methods, computational fluid dynamics, and reduction of test data can be used to develop simple lumped parameter models that have the same accuracy as the more complex models. These accurate lumps can then be used in the network analysis of a larger system without any run time penalty.

The relative effective thermal mass of the component varies with geometry and flow conditions. In this example, the relative effective thermal mass of the hydraulic actuator was only 10% when static but 25% when moving but for the hydraulic pump it was 100%. For the bellows reservoir it was 83% and for fittings 30%. Tube supports were less than 1% of the system and could be ignored. It was also found that the variable displacement pump case drain flow varied with temperature raised to the 4.4^{th} power ($T^{4.4}$).

ACKNOWLEDGEMENTS

The Subsystem Manager for the TVC system at Glenn Research Center is David Frate. The Product Lead is Robert Tornabene and the System Architect is Paul Solano.

REFERENCES

1. SINDA/FLUINT User's Manual: General Purpose Thermal/Fluid Network Analyzer, v5.3, C&R Technologies, Nov. 2009

CONTACT

For further information contact Robert Christie at
Robert.J.Christie@NASA.GOV
or 216-433-5249

NOMENCLATURE, ACRONYMS, ABBREVIATIONS

CFD	Computational Fluid Dynamics
DAC	Design Analysis Cycle
DCU	Data and Control Unit
ESC	Engine Start Command
FEM	Finite Element Method
F	Fahrenheit
GRC	Glenn Research Center
hr	Hour
J	Joule
LOX	Liquid Oxygen
LP	Lumped Parameter

MPS Main Propulsion System
MSFC Marshall Space Flight Center
PID Proportional Integral Derivative
TPA Turbine Pump Assembly
TVC Thrust Vector Control
US Upper Stage
W Watt

Appendix Ref. 1

SINAPS is a graphical user interface for SINDA/FLUINT. SINDA is used as the "equation solver" for the thermal network and FLUINT is the "fluid integrator" for the fluid network. In FLUINT the flow between lumps is represented by TUBES or connectors and the differential equation for TUBES, which is Newton's second law (F=m•a), is:

$$\frac{dFR_k}{dt} = \frac{AF_k}{TLEN_k}\left(PL_{up} - PL_{down} + HC_k + FC_k \cdot FR_k \cdot |FR|_k^{FPOW_k} + AC_k \cdot FR_k^2 - \frac{FK_k \cdot FR_k \cdot |FR|_k}{2 \cdot \rho_{up} \cdot AF_k^2}\right)$$

where

FR	Mass flow rate
TLEN	Tube length
AF	Flow area
PL	Lump pressure
HC	Head coefficient
FC	Irrecoverable loss coefficient
AC	Recoverable loss coefficient
FK	Additional K-factor losses

and for connectors the governing equation is:

$$\Delta FR_k^{n+1} = GK_k^n(\Delta PL_i^{n+1} - \Delta PL_j^{n+1}) + HK_k^n + EI_k^n \cdot \Delta HL_i^{n+1} + EJ_k^n \cdot \Delta HL_J^{n+1} + DK_k^n \cdot \Delta FR_t^{n+1}$$

where

GK	partial derivative of the flow rate with respect to (w.r.t.) pressure drop changes
HK	flow rat offset: difference between next FR and current, where next R is calculated assuming that the endpoint lumps do not change
EI	partial derivative of flow rate w.r.t. upstream enthalpy changes
EJ	partial derivative of flow rate w.r.t. downstream enthalpy changes
DK	partial derivative of flow rate w.r.t. its twin's flow rate (if twinned)

During the transient thermal analysis of the TVC hydraulic system the time-independent version of the TUBE was used, which is called a short tube or STUBE. The STUBE reacts instantaneously to flow forces, i.e. it has no inertia.